

## 2.1. Introduction

Instabilities or beam-wave interaction mechanism of a HPM sources can be understood with the interaction between the slow or fast space charge waves and the electromagnetic waves in the waveguiding structures. The slow space charge waves are referred as the waves with the phase velocities slower than the electron beam velocity in the propagation direction. On the other hand, the fast space charge waves are referred as the waves with phase velocities faster than the electron beam velocity. For high power microwave (HPM) generation in the slow wave device (MILO), study on the various condition of self magnetic insulation mechanism is taken into account to eliminate the requirement of the external DC magnetic field. This inherent property makes this device compact and reliable for defense purpose. HPM oscillators facilitated by the external electromagnets require two power sources which may also give rise to electrical breakdown problem as the higher voltages are approached. These oscillators (for example: magnetron) are having high inherent impedance that severely limits the output power level. Thus, for efficient operation at higher power levels, it would be desirable to have oscillator that operates at a lower impedance value and also eliminate the problem of voltage matching. Magnetically insulated line oscillator (MILO) is typically, reliable HPM source; which is a compact, stable and efficient microwave tube. Operation mechanisms and different parameters of gigawatt range source, MILO is similar to those of the relativistic magnetron. The prime difference is related to the phenomena of magnetic insulation. In magnetron, an external axial magnetic field is required for establishing magnetic insulation, on the other hand, the attractive feature of MILO that it works on the principle of self magnetic insulation for confining the electron flow and has low impedance that makes it suitable to operate at higher power levels. Thus, it is of interest to understand the

basic physics of self-magnetic insulation mechanism that pertains inside the MILO device. This study is speculates in this chapter, taking into account relativistic electron flow, presence of which significantly affect the microwave frequency and power level of the device. A number of independent research works have been reported in various literature for the analysis of the insulation mechanism considering presence of external magnetic field, incorporating different approaches [Hull (1921), Lovelace and Edward Ott (1974), Davidson *et al.* (1984), Tsang and Davidson (1986), Lawconnell and Neri (1989)]. The non-relativistic single particle analysis for magnetron was explained by Hull and the relativistic self-consistent cartesian treatment begun around 1973. Expressions for critical magnetic field, considering case of relativistic space-charge flow [Bergeron and Poukey (1975), Creedon (1975)]. During analysis, it is assumes that the total energy and canonical momentum across flow are conserved, known as Brillouin flow theory. In 1979, Mendel explained canonical momentum and energy profiles for flows across the electron sheath for a variety of electron orbits. Creedon and Wang extended the laminar Brillouin flow theory in the cylindrical coordinates system. For confining electron flow in coaxial geometry, magnetically insulated flow mechanism has been defined considering three different processes. First process named, self limited magnetically insulated flow, second is load limited magnetically insulated flow and third process named constant flux limited magnetically insulated flow. MILO operates on the principle of load limited magnetically insulated flow. During magnetic insulation, electron drift parallel to the cathode and an electron sheath is formed between the disc tip and cathode surface. This electron sheath equilibrium is known as the relativistic Brillouin flow (RBF). During RBF, all the electrons have same constant Hamiltonian and canonical momentum.

The present Chapter 2 of this thesis describes the operational theory and limitation of the relativistic magnetron and also discusses the features of RF resonant structure for MILO in comparison to the magnetron under consideration. Section 2.1 describes basics of MILO in conjunction with condition for explosive emission for relativistic device. This section also contributes to condition for magnetic insulation. Section 2.2 describes the EM field theory to discuss the condition for relativistic Brillouin flow. Mathematical expression for Hull cutoff condition and Buneman-Hartree condition and then Hull cutoff curve and Buneman-Hartree curve are also explained in this section. In next section, effect of axial disc periodicity on the expression for critical current is also presented.

### **2.1.1 Comparison between Magnetron and MILO**

Magnetically insulated line oscillator (MILO) is a linear magnetron variant that was invented to take advantage of very high current requirement of modern pulsed power systems. Both relativistic magnetron and MILO are HPM sources, but their working mechanisms differ in many ways. MILO is a linear device in which an azimuthal self-generated magnetic field created due to current flow in the device. Thus, it does not require axial external magnetic field as employed in magnetron for confining the electron flow. In MILO, generated RF propagates axially rather than azimuthally as in magnetron. MILO operates at constant drift velocity and therefore has no tuning requirements as for Magnetron. The magnetic field automatically adjusts to changing drive voltage, thus maintaining constant drift velocity. During MILO operation, axial drift velocity is proportional to the impedance which is virtually independent of voltage and is given by:

$$\frac{v_d}{c} = \frac{Z_p}{Z_0}.$$

$Z_p$  is the impedance of magnetically insulated line is almost independent of voltage and written as,  $Z_p = 23 \ln(r_a / r_c)$  and expression of drift velocity for magnetron is given by:

$$v_d = \frac{E \times B}{|B|^2} .$$

In magnetron, the space charge and diamagnetic effects of the electron layer cause E and B to vary with distance from the cathode, cause drift velocity to vary. The resonance requirement in crossed field devices is that drift velocity for some electrons must equal the phase velocity of an electromagnetic wave travelling in the same direction.

### 2.1.2 Basics of the MILO

MILO is a crossed field device, operates on the principle of magnetic insulation uses intense relativistic electron beam (IREB) for microwave generation, typically operates at conditions near relativistic Brillouin flow (RBF) which does not require external DC magnetic field. For the generation of relativistic beam current and gigawatt power level, cylindrical cathode structure follows the process of explosive emission condition.

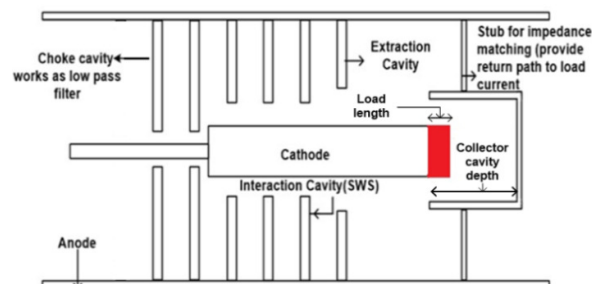


**Figure 2.1:** Schematic of a typical MILO device.

Typically, MILO consists of a cylindrical field emissive cathode surrounded by a number of coaxial metal discs as a slow wave RF interaction structure, few filter

discs forming the cavities towards input side and one extractor disc (cavity) toward output side along with the stub and collector refer to Figure 2.1. The load region of MILO comprises of the part of cathode inside collector (load length) and the collector cavity depth. Electron current flow through load side generates the required magnetic field which insulates the electron flow in the SWS region. Critical current required for the magnetic insulation is explained in next sub-section.

### 2.1.3 Condition for the Explosive Emission

As MILO is a high power device, high DC voltage is applied between cathode and anode, which causes explosive emission from the central cylindrical cathode surface due to expansion of cathode generated plasma, resulting in high beam current. Velvet cathode is often used for this device that acts as an explosive emitter. Materials implemented for explosive electron emission must have low electric field threshold for plasma initiation, emits uniformly, and has a low gap closure velocities. More detailed explanation is given in Chapter 6.

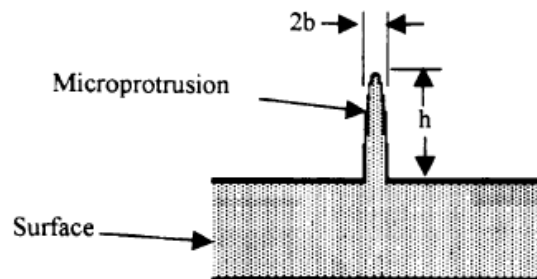


**Figure 2.2:** Explosive emission from cathode surface [Miller (1998)].

With the application of a large voltage, the field lines converge on the tip of the microprotrusion, enhancing the localized fields, enabling electrons to tunnel through

the decreased width of the potential barrier. The localized electric field at the tip can be expressed as:

$$E_{\text{local}} = f E.$$

In above expression,  $f$  is the field enhancement factor and  $E$  is the electric field in the absence of microprotrusion. The field enhancement factor can be written as [Miller (1998)]:

$$U_0 = \frac{(x^2 - 1)^{1.5}}{x \ln[x + (x^2 - 1)^{\frac{1}{2}}] - (x^2 - 1)^{\frac{1}{2}}}, \quad x = \frac{h}{b} \quad (x > 1) .$$

With the beginning of field emission, the flow of tunneling electrons increases the temperature of the microprotrusion due to Joule heating and eventually melts the whisker into a vapor state. On almost any cathode surface there exist microscopic surface protrusions (whiskers) which are typically on the order of  $10^{-4}$  cm in height with a base radius of less than  $10^{-5}$  cm and tip radius usually much smaller than the base radius. Whisker concentrations have ranged from 1 to  $10^4$  whiskers/cm<sup>2</sup> approximately.

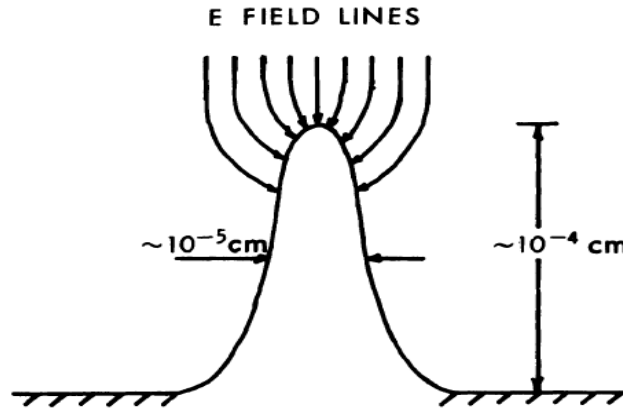


**Figure 2.3:** Microscopic view of the local electric field enhancement at the tip of a whisker-like protrusion on the cathode surface [Miller (1998)].

Application of an electric field leads to the appearance of a large negative surface charge density on the top of the microprotrusions and consequently, to a

significant enhancement (up to  $10^4$  times) of the local electric field. The enhanced electric field causes the intense electron field emission with current densities up to  $10^6$ – $10^7$  A/cm<sup>2</sup> [Krasik *et al.* (2000)]. This leads to a fast increase in the temperature of the individual emitters due to Joule heating. When an electric current flows through a solid with finite conductivity, energy is converted to heat through resistive losses in the material. The heat is generated on the microscale, when the conduction electrons transfer energy to the conductor atoms through collisions. At this moment, the electron field emission transforms to thermionic electron emission. Further, because of the extremely high electron current density, explosion of the top of the micro-protrusions takes place. This explosion process causes the formation of a neutral cloud which is simultaneously ionized by electrons, leading to the formation of plasma. This plasma can provide an electron current density up to hundreds of MA/cm<sup>2</sup>. However, the maximum electron current density is limited by the space-charge of the emitted electrons. These types of cathodes can be named “passive” cathodes because the plasma formation occurs under the application of the HV pulse. Therefore, it is extremely important that these cathodes provide uniform plasma simultaneously with the beginning of the accelerating pulse.

***Maximum temperature of the micro-point before it becomes explosive:***

The expression for the maximum value of  $T$  (at the tip of the emitter) is

$$T_{\max} = \frac{1}{2} \left( \frac{j^2 \rho}{k} \right) L^2$$

where,

$j$  = electron current density,

$\rho$  = electrical resistivity,

$k$  = thermal conductivity of material,

and

$L$  = length of micropoints.

Resistivity during explosive emission is calculated using expression for the plasma electrical conductivity and can be given by

$$\sigma_{dc} = \frac{n_e e^2}{m\nu}$$

where,

$$\nu = T^{-3/2},$$

$n_e$  = electron density,

$T_e$  = electron temperature,

and

$\nu$  = collision frequency which decreases with electron temperature.

For example, consider the case of tungsten, choosing intermediate values of  $\rho = 50 \times 10^{-6} \Omega \text{ cm}$  and  $k = 0.25 \text{ cal/sec cm } ^\circ\text{C}$  yields [Miller (1998)]:

$$T_{\max} = (2.5 \times 10^{-5}) j^2 L^2 (^\circ\text{C}).$$

where  $j$  is in  $\text{A/cm}^2$  and  $L$  is in centimetres. For typical whisker lengths of  $10^{-4}$  -  $10^3$  cm, the current density required to bring the tip of the whisker to the melting point ( $3400^\circ\text{C}$ ) is of the order of  $10^7$  -  $10^8 \text{ A/cm}^2$ .

#### **2.1.4 Condition for Magnetic Insulation and Critical current**

In high power device, high DC voltage is applied between cathode and anode, which causes explosive emission from the central cylindrical cathode surface, resulting in high relativistic current. The electron beam is initiated by explosive emission at the surface of a cylindrical velvet cathode. Due to self generated magnetic field, electrons in the beam can be insulated from the SWS [Cousin (2005)]. The self-azimuthal magnetic field generated due to the currents flowing in the system acts perpendicular to the electric fields to confine the electrons [Lawconnell and Neri (1989)]. When the currents (charging current, critical current, anode current) becomes appropriate, the self-magnetic field helps in confining electrons flow parallel to the cathode and greatly reduce the loss of electrons to the anode. When charging current becomes equal to the critical current, a magnetic cutoff condition



establishes in the interaction (RF) periodic structure and sustains the EM fields present in the interaction region. Now, due to the presence of crossed electric (radial) and magnetic (azimuthal) fields in the device, emitted electrons drift toward the axial ( $z$ ) direction of the structure, region between the cathode and the tip of metal coaxial discs with a velocity  $v_z$ . For the establishment of magnetic insulation condition, the electrons flow is generally relativistic and collisionless. Therefore, the relativistic Vlasov equation is used as a starting point for developing the physics of magnetic insulation. Writing  $z$  component of force equation in polar coordinate:

$$\frac{dp_z}{dt} = ev_r B_\theta .$$

Substituting relation for axial relativistic momentum and further rearranging, results in expression for critical current derived by [Dwivedi and Jain 2013] and is written as:

$$I_{cr} = \frac{I_0 \sqrt{\gamma_0^2 - 1}}{\ln(r_a / r_c)}, \quad I_0 = \frac{4\pi m_0 c^3 \epsilon_0}{e} = 17kA \text{ is the starting current.} \quad (2.2)$$

Critical current ( $I_{cr}$ ) is the minimum cathode current, needed to generate the self-magnetic field to create the insulation between the tip of disc and cathode. Expression for cut-off magnetic field can be written as:

$$B_c = \frac{\mu_0 I_{cr}}{2\pi r_c} = \frac{\mu_0 I_0 \sqrt{(\gamma_0)^2 - 1}}{2\pi r_c \ln(r_a / r_c)} .$$

Critical magnetic field is minimum magnetic field required for magnetic insulation to occur. Conditions of magnetic cut-off and interaction in the device are controlled by the load or critical current. Further, the load current is decided by the space between collector and cathode. The space between the collector and cathode is optimized in order to allow a maximum current, in the slow wave structure, for better interaction. Condition for magnetic insulation is being described in next section.

### 2.1.5 Parapotential or Anode Current Flow in the MILO

Anode current should be more than the minimum critical current required by the interaction structure to create sustained self-magnetic insulation. When the anode current is less than the critical current, all the electrons emitted by the cathode reaching the anode causes electrical breakdown between anode-cathode gap and no insulation occurs between tip of discs and cathode. When the anode current is more than critical current, all the electrons are grazed from the anode surface towards cathode. When charging current become equal to critical current, electrons are confined between tip of discs and cathode due to self-azimuthal magnetic field. This is the basic principle for producing very high-power microwave pulses in a HPM device MILO. The flow of electrons between cathode and tip of the metal disc can be described using relation

$$\frac{dp}{dt} = -e(E + v \times B) . \quad (2.3)$$

Writing Maxwell's law of electrostatic and magnetostatic as:

$$\nabla \cdot E = \frac{\rho}{\epsilon_0}, \quad \nabla \times B = \mu_0 J \quad . \quad (2.4)$$

Poisson equation can be written as:

$$\nabla^2 V = -\frac{\rho}{\epsilon_0} \quad .$$

For the relativistic Brillouin flow pattern, the electron trajectories are straight line along equipotential surfaces, so that  $dp/dt = 0$  thus, Equation (2.3) can be written as,

$$E = -v \times B \quad .$$

Taking divergence both sides,

$$\nabla \cdot E = \frac{-B \cdot (\nabla \times v)}{(1 - \beta^2)} \quad .$$

Using cylindrical coordinates in above equation and after rearranging, above equation can be written as [Dwivedi and Jain (2013)]:

$$\frac{1}{r} \frac{\partial}{\partial r} \left( r \frac{\partial V\{r\}}{\partial r} \right) = \gamma^2 \frac{\partial V\{r\}}{\partial r} \left( \frac{1}{v_z} \frac{\partial v_z}{\partial r} \right) \quad . \quad (2.4)$$

Using law of conservation of energy,  $(\gamma\{r\}-1)mc^2 = eV\{r\}$ , one can write:

$$\frac{\partial V\{r\}}{\partial r} = \frac{mc^2}{e} \frac{\partial \gamma\{r\}}{\partial r} \quad . \quad (2.5)$$

Substituting Equation (2.5) in (2.4), one gets differential equation that described parapotential flow, same as derived by [Lemke (1989)] as:

$$\frac{1}{r} \frac{\partial}{\partial r} \left( r \frac{\partial \gamma}{\partial r} \right) = \frac{\gamma}{\gamma^2 - 1} \left( \frac{\partial \gamma}{\partial r} \right)^2 \quad . \quad (2.6)$$

Above equation describe differential equation describing magnetic insulation and on solving this we get [Creedon (1975)]:

$$\ln(r) = C_1 \ln \left[ \gamma + (\gamma^2 - 1)^{\frac{1}{2}} \right] + C_2 \quad r_c \leq r \leq r_m \quad , \quad (2.7)$$

where  $\gamma_m$  is the value of  $\gamma$  at the insulated flow pattern, then the boundary condition for Equation (2.7) can be written in terms of  $r$ . At  $r = r_c$ ,  $\gamma(r_c) = 1$  and at  $r = r_m$ ,  $\gamma = \gamma_m$ . Satisfying these boundary conditions in Equation (2.7),  $C_2 = \ln(r_c)$  and

$$C_1 = \frac{\ln(r_m) - \ln(r_c)}{\ln \left[ \gamma_m + (\gamma_m^2 - 1)^{\frac{1}{2}} \right]} \quad . \quad (2.8)$$

To relate potential  $V_m$  at  $r_m$  to anode potential  $V_0$  at  $r_0$ , it is necessary to solve Laplace's equation in vacuum region between  $r_m$  and  $r_0$ . Set  $\rho = 0$  results in  $\nabla^2 V = 0$  then  $\nabla \cdot E = 0$  and making transformation from  $V$  to  $\gamma$  and from  $r$  to  $\ln(r)$  given by

$$\gamma = 1 + \frac{eV}{m_0 c^2} \quad \text{and} \quad \frac{d(\ln(r))}{dr} = \frac{1}{r} \quad , \quad \text{then results in} \quad \frac{d^2 \gamma}{d(\ln(r))^2} = 0 \quad \text{with solution}$$

$$\gamma = \frac{\gamma_0 (\ln(r) - \ln(r_m)) - \gamma_m (\ln(r) - \ln(r_0))}{\ln(r_0) - \ln(r_m)} \quad \ln(r_m) \leq \ln(r) \leq \ln(r_0) \quad (2.9)$$

where,  $\ln(r_0)$  and  $\gamma_0$  are the value of  $\ln(r)$  and  $\gamma$  at the anode.

Differentiating Equation (2.7) and Equation (2.9) setting  $\gamma = \gamma_m$  and equating the results gives:

$$C_1 = \frac{\ln(r_0) - \ln(r_m)}{\gamma_0 - \gamma_m} (\gamma_m^2 - 1)^{\frac{1}{2}}. \quad (2.10)$$

$\ln(r_m)$  can be expressed as a function of  $\gamma_0$ ,  $\gamma_m$  and  $\ln(r_c)$  by equating expression for  $C_1$  given by Equations (2.8) and (2.10) and then calculating value of  $\ln(r_m)$  and then substituting in Equation (2.10), we get:

$$C_1 = [\ln(r_0) - \ln(r_c)] / \ln[\gamma_m + (\gamma_m^2 - 1)^{1/2}] + (\gamma_0 - \gamma_m)(\gamma_m^2 - 1)^{-1/2} \quad (2.11)$$

Relation between the azimuthal magnetic field and current flowing is written as:

$$B_\theta = \frac{\mu_0 I\{r\}}{2\pi r}, \quad \text{also } E_r = v_z B_\theta.$$

On substituting above values,  $I\{r\} = \frac{E_r(2\pi r)}{\mu_0 v_z}$ , making transformation from  $v$  to  $\gamma$

and  $v_z$  by  $-\beta c$  gives,

$$I\{r\} = I_\alpha \frac{1}{\beta} \frac{d\gamma}{d(\ln(r))}, \quad (2.12)$$

where,

$$I_\alpha = \frac{2\pi m_0 c^2}{\mu_0 c e} = 8500A \quad .$$

Differentiating Equation (2.7), we get

$$\frac{d\gamma}{d(\ln(r))} = \frac{(\gamma^2 - 1)^{1/2}}{C_1} = \frac{\beta\gamma}{C_1} \quad (2.13)$$

Substituting Equation (2.13) in Equation (2.12), to get:

$$I\{r\} = I_\alpha \frac{\gamma}{C_1} \quad (2.14)$$

Total current flowing is given by putting  $\gamma = \gamma_m$  in above equation and combine with Equation (2.11),

$$I_0 = I_\alpha g \gamma_m \left[ \ln(\gamma_m + (\gamma_m^2 - 1)^{1/2}) + \frac{\gamma_0 - \gamma_m}{(\gamma_m^2 - 1)^{1/2}} \right], \quad (2.15)$$

where, 
$$g = \frac{1}{\ln(r_a / r_c)} .$$

Substituting  $\gamma = 1$  in Equation (2.14), it can be seen that part of total current must flow on the cathode surface or in the cathode plasma. Thus, charging current is given by Equation (2.15):

$$I_c = \frac{I_0}{\gamma_m} . \quad (2.16)$$

Part of the total current  $I_0$  that flows as an electron beam in the diode is  $I_e = I_0 - I_c$ . Combining Equations (2.15) and (2.16), it can be shown that this beam current is maximum when  $\gamma_m = \gamma_0$ . Corresponding current is known as saturated parapotential current and is calculated by setting  $\gamma_m = \gamma_0$  in Equation (2.15) to get:

$$I_p = I_\alpha g \gamma_0 \ln \left[ \gamma_0 + (\gamma_0^2 - 1)^{1/2} \right] . \quad (2.17)$$

From Equations (2.15) and (2.16), it can be shown that (for a fixed value of  $\gamma_0$  and  $g$ ),  $I_c$  is minimum when  $I_0 = I_p$ .

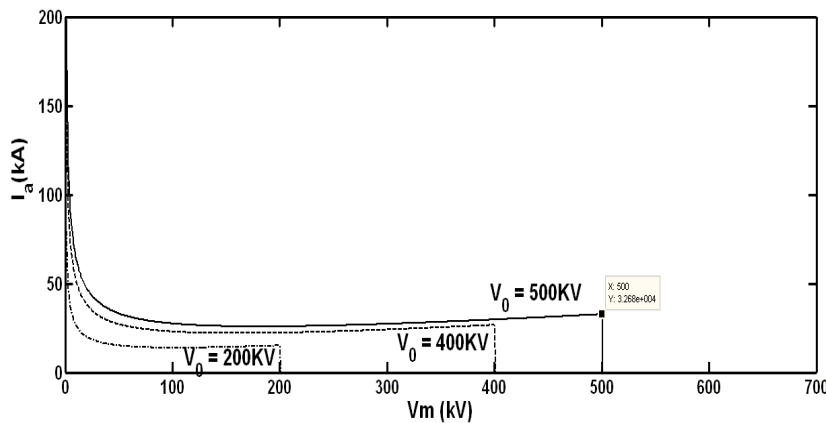


**Figure 2.4:** Variation of parapotential current  $I_p$  versus  $V_m$  (maximum developed potential). Here  $V_m = V_0$  and  $I_0 = I_p$ .

## 2.2 Condition of Relativistic Brillouin Flow and Magnetic Insulation

R. C. Davidson and K. T. Tsang (1986) describe the equilibrium properties of relativistic electron flow in planar diode configuration. This section describes the equilibrium properties of relativistic electron flow along the insulated sheath for cylindrical diode configuration of MILO. During MILO operation, when its charging current becomes equal to the critical current, a magnetic cutoff condition establishes in the RF periodic structure and sustains the EM fields present in the interaction region. This section mainly explains the condition for magnetic insulation in MILO. This condition is being derived here taking into account formation of plasma on the cathode surface due to explosive emission that creates high density electron beam. Application of high voltage DC pulse between cathode and anode causes electrons emission from the cylindrical cathode surface. The electrons are field emitted from the cold cathode by the process termed as explosive electron emission. This type of emission results in the formation of non-neutral plasma sheath which is a good source of electron emitter [Hilsabeck and O'Neil (2001)]. Electro-magneto dynamics equation and momentum conservation lead to complete description of the magnetically insulated flow. During analysis it has been assumed that equilibrium is represented by relativistic Laminar flow in crossed electric and magnetic fields, with space charge limited emission.

The equilibrium configuration is shown in Figure 2.5. In the present section, conditions for the RBF flow are studied, considering the  $(E \times B)$  drift of a relativistic electron beam in the region between the cathode and anode. Electro-magneto

dynamics equation and momentum conservation lead to complete description of the magnetically insulated flow.

A radial electric field  $E_r$  gets established due to applied DC potential between explosive emissive cathode and anode. Gauss's Law in cylindrical coordinate is written as [Levy (1965)]:

$$\frac{1}{r} \left( \frac{\partial}{\partial r} (rE) \right) = \frac{en_e\{r\}}{\epsilon_0},$$

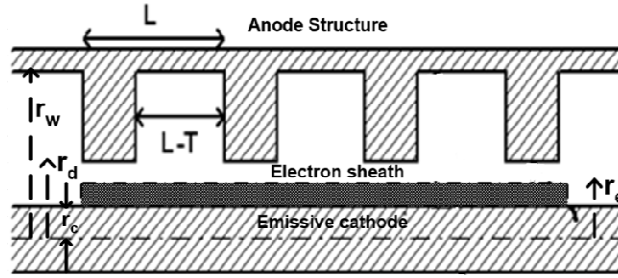


**Figure 2.5:** Schematic of RF interaction structure.

where  $n_e\{r\}$  is the electron density in the radial direction. Considering property of electric field at cylindrical charged surface and space charge limited emission ( $E_r = 0$  ( $r=r_c$ )), above Equation can be written as:

$$\frac{\partial E_r}{\partial r} = \frac{en_e\{r\}}{\epsilon_0}. \quad (2.18)$$

Differential form of Ampere's law in cylindrical coordinates is written as,

$$\frac{1}{r} \left( \frac{\partial}{\partial r} (rB_\theta) \right) = \mu_0 n_0 e v_z .$$

Initially during electron emission, no azimuthal component is present,  $B_\theta / r = 0$  in above expression,

$$\frac{\partial B_\theta}{\partial r} = \mu_0 en_0 v_z .$$

Substituting  $J = \rho v$  and  $\mu_0 = 1/(\epsilon_0 c^2)$  in the above equation, we get:

$$\frac{\partial B_\theta}{\partial r} = en_e\{r\}v_z / (\epsilon_0 c^2). \quad (2.19)$$

This self magnetic field redirects electrons back towards the cathode due to  $(v \times B)$  force. Thus, electrons get drift in  $z$  direction with the velocity  $v_z$ . Under the influence of electromagnetic forces, the momentum equation can be written as

$$\dot{p}_r = eE_r\{r\} - ev_z B_\theta\{r\} \quad . \quad (2.20)$$

Electrons present on the plasma sheath which results due to explosive emission from the cathode surface evolve or rotate at a velocity  $\dot{\theta}\{r\}$  [Tsang and Davison (1985)]. Relativistic electron beam (charging current) results in the self azimuthal magnetic field at which magnetic insulation takes place as a specific condition. For magnetic insulation condition to occur, the centrifugal force must be balanced by the Lorentz force such that,

$$\frac{e}{\gamma}[E_r + r\dot{\theta}B_\theta] = mr\dot{\theta}^2 \quad .$$

Introducing relativistic cyclotron frequency,  $\omega_c = eB_\theta / \gamma m_e$  and relativistic plasma frequency,  $\omega_p = ne^2 / \gamma m_e \epsilon_0$ , the angular speed satisfied quadratic equation:

$$\dot{\theta}^2 + \omega_c \dot{\theta} + qE_r / m_e r = 0 \quad .$$

Here,  $q = \omega_p^2 / \omega_c^2$ , represents parameter that limits instability along the magnetically insulated sheath. Existence of this condition results in drift of the each electron along  $z$  direction at drift velocity  $v_z = E_r / B_\theta$ . Thus, insulated sheath follows condition of RBF equilibrium.

For the electrons streaming parallel to the  $z$ -axis, radial momentum will be zero and drift velocity of the relativistic electron beam can be written as  $v_z = E_r / B_\theta$  [ Dwivedi and Jain (2013)]. Substituting value of  $v_z$  and  $n_e\{r\}$  from Equation (2.18) into Equation (2.19), then



$$c^2 \frac{\partial B_\theta^2\{r\}}{\partial r} = \frac{\partial E_r^2\{r\}}{\partial r}. \quad (2.21(a))$$

Integrating above Equation, within limits of the space charge electric field and the self magnetic field  $B_\theta$  generated by the beam, one gets:

$$B_\theta^2\{r\} - \frac{E_r^2\{r\}}{c^2} = \text{constant} = w. \quad (2.21(b))$$

Under RBF condition, the canonical momentum and total energy across the electron sheath become zero [Lemke (1989)]. From above equation (2.21),  $c^2 B_\theta^2\{r\} - E_r^2\{r\}$  represents equilibrium condition establishes during the magnetic insulation and is equal to a constant quantity, imposing the boundary condition  $r_c \leq r \leq r_e$ . Thus, the drift velocity will modify the relativistic mass factor  $\gamma$  along the electron sheath:

$$\gamma\{r\} = \frac{1}{\sqrt{1 - v_z^2/c^2}} = \frac{1}{\sqrt{1 - E_r^2\{r\}/c^2 B_\theta^2\{r}}} . \quad (2.22)$$

Substituting Equation (2.21) in Equation (2.22),

$$B_\theta\{r\} / \gamma\{r\} = \sqrt{w} = \text{constant} . \quad (2.23)$$

Equations (2.21) and (2.23) define the stable equilibrium condition for the relativistic electron flow (RBF) in crossed electric and magnetic field. Multiplying both side of Equation (2.21(a)) by  $r^2$ , Equation can be rewritten as,

$$[r^2(E^2 - (cB)^2)]' = 0 .$$

Integrating above Equation from cathode radius  $r_c$  to some arbitrary  $r_e$  (radius of insulated electron sheath) [Lawconnell and Neri (1990)],

$$r_e^2[E_e^2 - (cB_m)^2] - r_c^2[E_c^2 - (cB_c)^2] = 0. \quad (2.24)$$

Considering space charge limited emission condition ( $E_c = 0$ ) and writing above equation in terms of anode and cathode currents, considering  $B_m = \frac{\mu_0 I_a}{2\pi r_e}$  and can be

written as [Lawconnell and Neri (1990)],

$$E_e = -\frac{c\mu_0}{2\pi r_e} (I_a^2 - I_c^2)^{\frac{1}{2}}. \quad (2.25)$$

$E_e$  represents electric field developed at the electron sheath. In above equation,  $B_m$  represents magnetic field along the electron sheath. During RBF, total energy of the electrons remains conserved along the electron sheath [Lemke (1989)],

$$(\gamma\{r\}-1)m_0c^2 - e\phi_0\{r\} = \text{constant} . \quad (2.26)$$

Now, imposing the boundary condition, at the cathode surface,  $\gamma(r=r_c) = 1$  and  $\phi_0(r=r_c) = -V_0$ , above Equation can be written, after solving constant value, after rearranging,

$$(\gamma\{r\}-1)m_0c^2 - e\phi_0\{r\} = eV_0. \quad (2.27)$$

Total energy of electrons is expressed using Equation (2.27). Differentiating the above expression with respect to  $r$ :

$$\frac{\partial\gamma}{\partial r} = \frac{e}{m_0c^2} \frac{\partial\phi_0\{r\}}{\partial r} .$$

Substituting  $\partial\gamma/\partial r$  from (2.22) and  $\partial\phi_0/\partial r = -E_r$  in above equation:

$$\gamma^3\{r\} \frac{E_r\{r\}}{B_\theta\{r\}} \frac{\partial}{\partial r} \left[ \frac{E_r\{r\}}{B_\theta\{r\}} \right] = -\frac{e}{m} E_r\{r\} .$$

Expanding the above using equations (2.19) and rearranging,

$$\left[ \frac{eB_\theta\{r\}}{m_0\gamma\{r\}} \right]^2 = \frac{e^2 n_e\{r\}}{m_0 \epsilon_0 \gamma\{r\}} \Rightarrow \omega_c = \omega_p . \quad (2.28)$$

In above Equation (2.28),  $\omega_c$  and  $\omega_p$  represent relativistic cyclotron and plasma frequencies, respectively [Davidson and Tsang (1984)]. Equation (2.28) represents condition of relativistic Brillouin flow ( $r_c \leq r \leq r_e$ ) for achieving magnetic insulation condition due to explosive emission process. It is under the action of above defined electromagnetic fields that magnetic cut off is reached inside the structure. Imposing condition (2.23) into expression (2.28), then rearranging, results

$$n_e\{r\}/\gamma\{r\} = (\epsilon_0/m_0)\omega = \text{constant} , \quad \text{for } r_c \leq r \leq r_e . \quad (2.29)$$

To ensure the formation of magnetically insulated sheath and fulfilling the RBF flow condition, the ratio of electron density to azimuthal magnetic field must also be equal to a constant and can be explained using Equations (2.23) and (2.29):

$$n_e\{r\} / B_\theta\{r\} = \text{constant} = (\varepsilon_0 / m_0) \sqrt{w} . \quad (2.30)$$

Now, differentiating (2.19) with respect to radius  $r$  and then substituting in (2.18) using property (2.30), yields [Tsang *et al.* (1985), Davidson *et al.* (1984)]:

$$\frac{\partial^2 B_\theta\{r\}}{\partial r^2} - s^2 B_\theta\{r\} = 0 , \quad (2.31)$$

where,

$$s^2 = \frac{\omega_p^4\{r_e\}}{\omega_c^2\{r_e\} c^2} = \frac{\omega_b^2\{r_e\}}{c^2}; \quad \omega_D\{r\} = \frac{\omega_p^2\{r\}}{\omega_c\{r\}} . \quad (2.32)$$

Here,  $\omega_D$  represents Diocotron frequency and  $s$  represents electromagnetic field strength along the magnetically insulated sheath. Solution of Equation (2.31):

$$B_\theta\{r\} = M \cosh(sr) + N \sinh(sr) ,$$

where,  $M$  and  $N$  are the integration constants and can be computed on applying boundary conditions at  $r = r_c$ , the above expression becomes [K. T. Tsang and R. C. Davidson (1986)]:

$$B_\theta\{r\} = B_c \frac{\cosh(sr)}{\cosh(sr_e)} , \quad r_c \leq r \leq r_e \quad (2.33)$$

and

$$B_\theta\{r\} = B_c , \quad r_e \leq r \leq r_d . \quad (2.34)$$

In this regard, using equilibrium properties, above magnetic field expressions (2.33) and (2.34) emphasizes the self-azimuthal magnetic field in the two structure regions.  $B_c$  represents the critical self magnetic field at the anode due to which electrons just graze the anode surface. During RBF, expression for electron density can also be calculated using equations (2.30) and (2.33), as:

$$n_e\{r\} = n_e^0 \frac{\cosh(sr)}{\cosh(sr_e)} , \quad (2.35)$$

where  $n_e^0$  is the electron density at boundary  $r = r_e$ . Considering Equations (2.23) and (2.31), the expression for the relativistic factor can be written as,

$$\gamma = \cosh(sr) . \quad (2.36(a))$$

Substituting Equation (2.35) in (2.18) after integrating results in expression for electric field and can be written as:

$$E_r(r) = -\frac{en_e^0 \sinh(sr)}{\epsilon_0 s \cosh(sr_e)} = -cB_c \frac{\sinh(sr)}{\cosh(sr_e)} . \quad (2.36(b))$$

Velocity for drift electrons is given by:  $v_z(r) = c \tanh(sr)$

Considering RBF or insulation condition (2.28), expression for the self azimuthal magnetic field can be written as:

$$B_\theta\{r\} = [n_e\{r\}m_e / \epsilon_0]^{1/2} .$$

Substituting above expression in Equation (2.33) and substituting value of critical magnetic field  $B_c = \mu_0 I_{cr} / 2\pi r_c$ , further recasting results in expression for critical current:

$$I_{cr} = \left[ \frac{n_e\{r\}m_e}{\epsilon_0} \right]^{1/2} \left[ \frac{\cosh(sr_e)}{\cosh(sr)} \right] 2\pi r_c \epsilon_0 c^2 . \quad (2.36(c))$$

Expression (2.36(c)) represents expression for critical current considering explosive emission from the cathode surface.

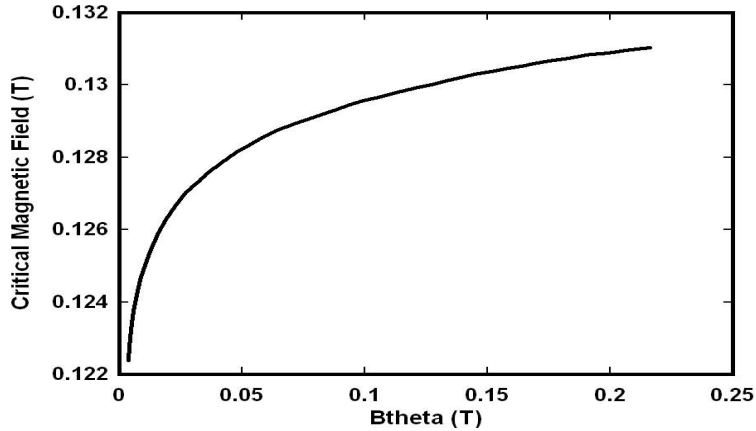


**Figure 2.6:** Variation of self azimuthal magnetic field with critical magnetic field.

In above figure,  $B_\theta$  is azimuthal self magnetic field at the anode during magnetic insulation due to which electrons just graze the anode surface. It is inferred from figure, at about when critical magnetic field become equal to  $B_{\text{theta}}$  (0.13T), magnetic insulation occurs and electrons drift in axial direction.

### 2.2.1 Hull cut-off and B-H condition

Hull cut-off represents the magnetic insulation condition, the minimum magnetic field required to prevent the emitted electrons from reaching the anode and in MILO this condition occurs when charging current becomes equal to critical current. Substituting expression for relativistic factor from Equation (2.36) in (2.27), resulting potential of the structure is defined as:

$$[\cosh\{sr\} - 1] = \frac{e}{m_0c^2}(V_0 + \phi_0\{r\}) \quad 0 \leq r \leq r_e \quad . \quad (2.37)$$

Differentiating Equation (2.37) with respect to  $r$ ,

$$\frac{\partial \phi_0\{r\}}{\partial r} = \frac{sm_0c^2}{e} \sinh\{sr\} \quad . \quad (2.38)$$

At the electron sheath, potential can be expressed as,

$$\phi_0\{r\} - \phi_0\{r = r_e\} = -E_r\{r_e\}(r - r_e) \quad . \quad (2.39)$$

Substituting Equation (2.38) in (2.39), substituting  $E_r = d\phi/dr$

$$\phi_0\{r\} - \phi_0\{r = r_e\} = -\frac{m_0c^2}{e} s(r - r_e) \sinh\{sr_e\} \quad . \quad (2.40)$$

Differentiating above with respect to  $r$ ,

$$\frac{\partial \phi_0(r)}{\partial r} = \frac{sm_0c^2}{e} \sinh(sr) \quad .$$

With respect to above defined potential, radial electric field at insulated sheath due to space charge effect [Lemke (1989)]:

$$E_r = -\frac{sm_0c^2}{e} \sinh(sr) \quad .$$

Considering continuity of electric field between different regions, potential in the region  $r_e \leq r \leq r_d$ , can be obtained using Equations (2.37) and (2.40),

$$\frac{e}{m_0 c^2} (V_0 + \phi_0\{r\}) = [\cosh\{sr_e\} - 1] + s(r - r_e) \sinh\{sr_e\} \quad . \quad (2.41)$$

It is desirable to couple  $B_c$  to the initial magnetic field strength  $B_\theta(r)$  developed between anode and cathode prior to the formation of Brillouin layer. This can be done by taking into account conservation of magnetic flux theorem, dividing structure into two regions, i)  $r_c \leq r \leq r_e$  and ii)  $r_e \leq r \leq r_d$ ,

$$\int_{r_c}^{r_d} B_\theta dr = \int_{r_c}^{r_e} B_c \frac{\cosh\{sr\}}{\cosh\{sr_e\}} dr + \int_{r_e}^{r_d} B_c dr \quad (2.42)$$

Solving above integral for these two regions, as shown in Figure 2.5, and substituting  $B_c = B_0 \cosh\{sr_e\}$  Equation (2.42) can be rewritten as,

$$\frac{eB_0}{m_0 c s} [\sinh\{sr_e\} + s(r_d - r_e) \cosh\{sr_e\}] = \frac{e}{m_0 c} B_\theta d \quad . \quad (2.43)$$

In above equation,  $B_0$  represents magnetic field developed due to the flow of parapotential or anode current. Drift electrons have motion along equipotential surface, thus total current is known as parapotential or anode current which is a function of the structure geometry and applied potential.

$$I_p = \frac{I_0}{2 \ln(r_d / r_c)} \gamma_0 \ln[\gamma_0 + (\gamma_0^2 - 1)^{1/2}] \quad .$$

During RBF flow,  $\omega_p = \omega_c$  and  $\gamma(r = r_c) = 1, s = \omega_p / c$ , Equation (2.43) can be written as,

$$\frac{eB_\theta r_d}{m_0 c} = \sinh\{sr_e\} + s(r_d - r_e) \cosh\{sr_e\} \quad . \quad (2.44)$$

Considering,  $r_e$  tends toward  $r_d$ , one obtains, potential in region  $r_e \leq r \leq r_d$ ,

$$\left( \frac{eB_\theta r_d}{m_0 c} \right)^2 = \cosh^2\{sr_d\} - 1 \quad . \quad (2.45)$$

When  $r_e = r_d$  and  $\phi_0\{r_d\}=0$ , Equation (2.37) can be written as,

$$\frac{eV_0}{m_0 c^2} = \cosh\{sr_d\} - 1 . \quad (2.46)$$

Substituting Equation (2.45) in (2.46), potential of the structure can be expressed as:

$$\frac{eV_H}{m_0 c^2} = \left[ 1 + \left( \frac{eB_\theta r_d}{m_0 c} \right)^2 \right]^{1/2} - 1 . \quad (2.47)$$

Above expression represents cut-off condition for MILO. Potential corresponding to this case is called Hull cut-off voltage. Equation (2.47) linked potential of the structure to the resultant total self magnetic field and defines Hull cut off voltage at specific condition of the magnetic insulation. When magnetic field is above cut off condition, there is an empty space between tip of the discs and electron sheath, where Equation (2.41) satisfies for the potential. At  $r = r_d$ ,  $\phi(r_d) = 0$ , Equation (2.41) can be written as:

$$\frac{eV_0}{m_0 c^2} = [\cosh\{sr_e\} - 1] + s(r_d - r_e) \sinh\{sr_e\} . \quad (2.48)$$

Combining equation (2.48) with equation (2.44), one obtains:

$$\frac{eV_0}{m_0 c^2} = [\cosh\{sr_e\} - 1] + \frac{eB_\theta r_d}{m_0 c^2} c \tanh\{sr_e\} - \frac{[\cosh^2\{sr_e\} - 1]}{\cosh\{sr_e\}} . \quad (2.49)$$

Since  $\gamma_0 = \cosh\{sr_e\}$ , we can easily verify that  $v_z = c \tanh\{sr_e\}$ . Also require that  $v_z = \beta_\rho c$  at the threshold voltage  $V_{BH}$ , we get the expression for the new potential when synchronism between the phase velocity of desired mode of the structure and the velocity of the drift electrons exist, on rearranging this equation:

$$\frac{eV_{BH}}{m_0 c^2} = \frac{eB_\theta r_d}{m_0 c^2} v_\phi - \left[ 1 - \left( 1 - \frac{v_\phi^2}{c^2} \right)^{1/2} \right] . \quad (2.50)$$

Above expression defines the limiting condition at which the beam interacts with the RF interaction structure. When the EM waves in the RF periodic structure are sufficient slowed down to allow synchronism with velocity of the drift electrons:

$$\frac{e}{m_0 c^2} V_{BH} \approx \frac{e}{m_0 c^2} B_\theta dv_\phi . \quad (2.51)$$

Expression defines the limiting condition for which the beam interacts with the anode structure and same as expressed by [Lau *et al.* (1987)]. When the electromagnetic waves in the anode structure called periodic structure are sufficiently slowed down to allow synchronism with the velocity of the drift electrons.

Thus potential grows in a linear manner with the magnetic field in the structure. Condition given in Equation (2.51) represents Bunemann-Hartree condition. For steady Brillouin flow, inequality  $V < V_H$  should exist to assure magnetic insulation of electron flow from contact with anode at  $r = r_e$ . Condition  $V > V_{BH}$  should sustain for interaction of outer electrons with the wave field for specified voltage. To identify the region of operation and oscillation condition, expressions for Hull cut-off voltage as well as Bunemann-Hartree condition for beam wave synchronism are derived above. Bunemann-Hartree voltage is the voltage at which oscillations should start provided at the same time magnetic field is sufficiently large so that undistorted space charge does not extend to the anode. For voltages less than Bunemann-Hartree threshold, the MILO will be non-resonant and it will not radiate microwave. The region of operation can be emphasized between the two conditions. Efficient operation generally occurs near the B-H threshold. The two conditions are proportional and their ratio is a function of only the voltage and phase velocity of the resonant wave.

From Figure 2.7, it could be concluded that for resonant condition in MILO, voltage must be greater than Bunemann-Hartree threshold ( $V_{BH}$ ) and less than that of Hull cut-



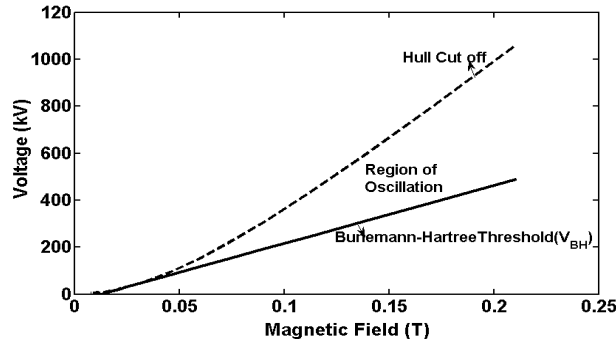


**Figure 2.7:** Graph showing region of oscillation in MILO.

off voltage ( $V_H$ ). During RBF flow, drift electrons have motion along equipotential surface, thus total current is known as parapotential or anode current.

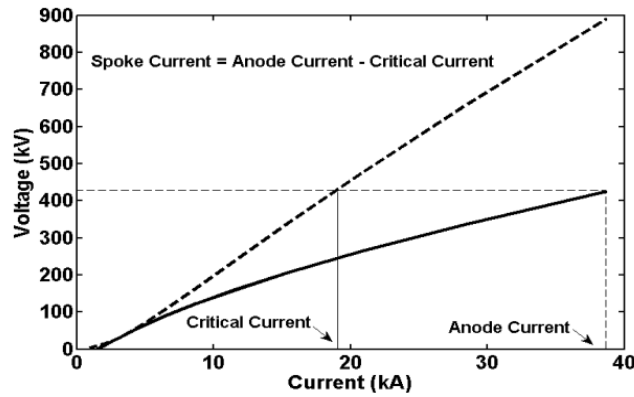


**Figure 2.8:** Operating voltage versus current.

Existence of various operating currents that are responsible for magnetic insulation and beam wave interaction mechanism at specified voltage can be determined from above Figure 2.8.

## 2.2 Operating Mechanism of MILO

For further study of beam-wave interaction mechanism, after the formation of electron sheath and RBF flow, now consider the profile function for RBF [Lemke (1989)],

$$f\{r\} = \frac{\sinh[A_n \ln(r/r_c)]}{\sinh[A_n \ln(r_e/r_c)]}$$

As derived in the previous section,  $E_e$  represents electric field developed at the electron sheath that further plays an important role during beam-wave interaction [Lawconnell and Neri (1990)],

$$E_e = -\frac{c\mu_0}{2\pi r_e}(I_a^2 - I_c^2)^{\frac{1}{2}}.$$

Electric flux along the electron sheath is written using Gauss law,  $\phi_e = E_e \cdot 2\pi rL$ , also  $\phi_e = q / \epsilon_0$ , thus relationship between electron charge per unit length ( $\sigma$ ) and electric field,

$$\sigma = 2\pi\epsilon_0 r_e E_e \quad \text{and} \quad v_d \sigma = (I_a - I_c). \quad (2.52)$$

$v_d$  represents average drift velocity of electron flow due to space charge effect that is necessary for establish synchronism condition. Substituting value of ( $\sigma$ ), results in expression for electric field along the insulated sheath. Thus, referring Equation (2.52), the previous equation for  $E_e$  can be recast in terms of drift velocity as:

$$E_e = \left[ \frac{(I_a - I_c)}{2\pi\epsilon_0 r_e v_d} \right] \hat{r}. \quad (2.53)$$

From Equations (2.51) and (2.53), expression for drift velocity can be written as,

$$v_d = c \left( \frac{I_a - I_c}{I_a + I_c} \right)^{1/2}. \quad (2.54)$$

Fraction of beam current in magnetic cutoff migrates towards the anode without passing by load and characterizes the leakage or escape current. This current contributes during the formation of spokes.

$$I_{escape} = I_a - I_c.$$

In above expression ( $I_a - I_c$ ) represents amount of RF current in MILO. Thus electric field at the anode is given by,

$$E_a = \frac{r_e E_e}{r_a} . \quad (2.55)$$

### 2.2.3 Beam-Wave Interaction Mechanism

MILO operates on the principle of magnetic insulation. During magnetic insulation an insulated electron sheath is formed between metal discs tip and cathode. Electrons present along the insulated sheath attain relativistic cyclotron and plasma frequency. Due to presence of axial and radial electric field, electrons present at the sheath boundary will undulate under the perturbing field, represents space charge waves. Oscillations due to these space charge waves led to instability, known as Diocotron instability that occurs in unneutralised charge sheets in the presence of uniform magnetic field.

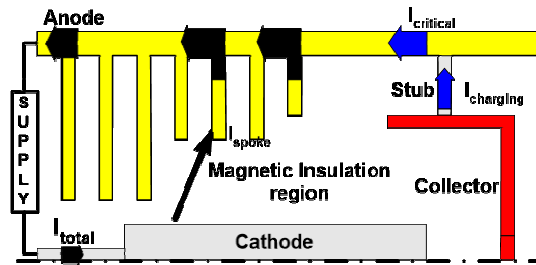


**Figure 2.9:** Schematic of MILO representing flow of current.

Diocotron instability pertains due to charges present on the plasma sheath, slip parallel to sheath surface which results in the generation of the space charge fields. This instability induces noise inside the cavities which oscillates at fundamental mode. This oscillation induces RF voltage inside the cavities. Electrons undulate in the form of spokes due to escape current when synchronism condition takes place. Thus for efficient beam-wave interaction mechanism, drift velocity of beam electrons must be equal to phase velocity of RF wave. Electric flux along the electron sheath is written using Gauss law,  $\phi_e = E_e \cdot 2\pi rL$ , also  $\phi_e = q / \epsilon_0$ , thus relationship between

electron charge per unit length ( $\sigma$ ) and electric field,  $\sigma = 2\pi\epsilon_0 r_e E_e$  and  $v_d \sigma = (I_a - I_c)$ .  $v_d$  represents average drift velocity of electron flow due to space charge effect that is necessary for establish synchronism condition. Substituting value of  $\sigma$ , results in expression for electric field along the insulated sheath [Lawconnell (1998),

$$E_e = \left( \frac{I_a - I_c}{2\pi\epsilon_0 r_e v_d} \right).$$

Difference between anode and cathode current is known as RF current or leakage current due to the space charge effect. Above condition represents non-linear phase operation in the MILO. In above equation,  $(I_a - I_c)$  represents leakage or escape current. Electric field derived above, develop across the charge layer generates a velocity shear or “slipping stream” in the layer and this phenomena leads to instability known as Diocotron instability. In this configuration, the transient state makes it possible to induce an RF wave in the SWS which grows in the  $\pi$  mode. Those space charge waves whose phase velocity is in near synchronism with the drift velocity of the beam contribute to spoke formation. RF emission becomes possible, when synchronism between the velocity of drift electron and the phase velocity of RF wave occurs, then only energy exchange takes place. Thus fraction of beam current in magnetic cutoff migrates towards the anode without passing to the load, that further characterized as “escape current” being accompanied by bunches of the electron beam called spokes. Considering RBF density profile, in this section author explain expression for magnetic field induction along radial direction and velocity of electrons along radial direction. Integrating above Equation (2.24) from cathode radius  $r_c$  to some arbitrary  $r_d$ , considering space charge limited emission ( $E_c = 0$ ),

$$(r_d E)^2 + (r_c c B_c)^2 = (r_d c B)^2. \quad (2.56)$$

Consider relationship between electron charge per unit length ( $\sigma$ ) and electric field,

$$\sigma = 2\pi\epsilon_0 r_e E_e, \quad (2.57)$$

where  $E_e$  is electric field at the electron sheath radius  $r_e$ . Gauss law in integration form is written as [Lawconnell and Neri (1990)]:

$$r_d E = \frac{1}{\epsilon_0} \int_{r_c}^r \rho r dr. \quad (2.58)$$

Lets represents total charge ( $q$ ) in the electron sheath per unit length as,

$2\pi \int_{r_c}^{r_m} \rho(r) r dr$ , also using Equation (2.57), then substituted in above equation,

$$\begin{aligned} rE &= \frac{2\pi}{\sigma} r_e E_e \int_{r_c}^r \rho(r) r dr \\ \Rightarrow rE &= r_e E_e \frac{\int_{r_c}^r \rho(r) r dr}{\int_{r_c}^{r_m} \rho(r) r dr} = r_e E_e f(r). \end{aligned} \quad (2.59)$$

$f(r)$  is normalized weighted density profile. From equation (2.56),

$$rE = [(r_m c B_m)^2 - (r_c c B_c)^2]^{\frac{1}{2}} f(r). \quad (2.60)$$

Also, 
$$v(r) = -\frac{E}{B}. \quad (2.61)$$

Writing above equation in terms of anode and cathode currents, considering

$$B_m = \frac{\mu_0 I_a}{2\pi r_e} \quad \text{and} \quad B_c = \frac{\mu_0 I_c}{2\pi r_c} \quad \text{we get:}$$

$$v(r) = c \left\{ \frac{(I_a^2 - I_c^2) f(r)^2}{[I_c^2 + (I_a^2 - I_c^2) f(r)^2]} \right\}^{1/2} \hat{z}, \quad (2.62)$$

where  $I_a$  is anode current and  $I_c$  is cathode current. Expression for relativistic factor at the electron sheath can be written as [Lawconnell and Neri (1990)]:

$$\gamma_e = \frac{I_a}{I_c}. \quad (2.63)$$

Brillouin density profile can be represented as [Lemke 1987],

$$\rho(r) = -\left(\frac{mc^2 \epsilon_0}{e}\right) \left(\frac{A_n^2}{r^2}\right) \cosh\left[A_n \ln\left(\frac{r}{r_c}\right)\right]. \quad (2.64)$$

$$A_n = \frac{1}{2} (\ln((1 + \beta_e)/(1 - \beta_e))) / \ln(r_e / r_c)$$

Using above expression Brillouin density profile,  $f(r) = \int_{r_c}^r \rho(r) r dr / \int_{r_c}^{r_m} \rho(r) r dr$  which is

the normalized weighted density profile can be expressed as [Lawconnell and Neri (1990)]:

$$f(r) = \sinh[A_n \ln(r / r_c)] / \sinh[A_n \ln(r_e / r_c)]. \quad (2.65)$$

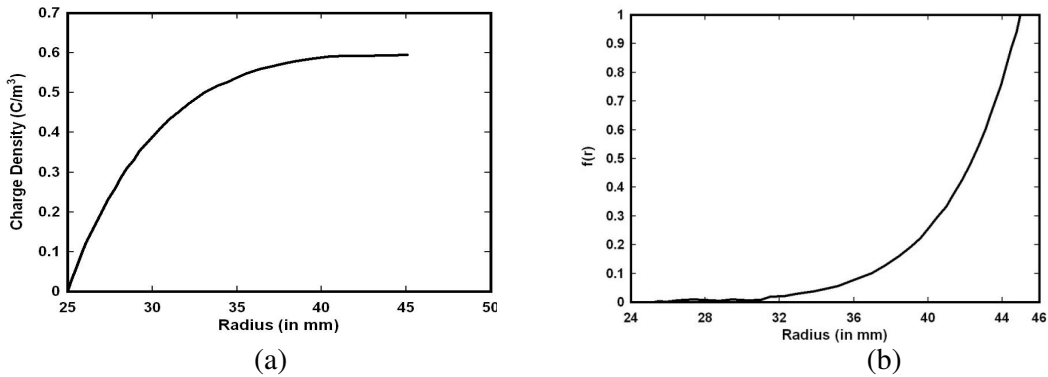


**Figure 2.10:** (a) Variation of charge density profile from cathode radius to disc radius, (b) Variation of normalized RBF profile with radius.

It can be inferred from Figure 2.10 (a), that initially electrons accelerates having some charge from cathode radius (25 mm), then varies linearly and after some time around radius (35 mm), electrons drift in axial direction and electron sheath is formed having charge density shown in Figure. Information regarding spoke formation can be realized from Figure 2.10 (b), from which it can be shown that due to instability along the sheath radius (35 mm), electrons escape towards the discs. Using charge density  $\rho\{r\}$  and velocity, the current density can be expressed as,

$$j\{r\} = \rho\{r\}v\{r\} . \quad (2.66)$$

Considering displacement current present between tip of discs and cathode surface due to presence of electric field along the insulated sheath, using Maxwell's Ampere's equation, corresponding magnetic induction is written as,

$$B\{r\} = \frac{\mu_0}{r} \left( \int_{r_c}^r j\{r\} dr + \frac{I_c}{2\pi} \right). \quad (2.67)$$

Using expression for current density, rearranging above expression can be written as,

$$B\{r\} = \left( \frac{\mu_0 I_c}{2\pi r} \right) \left\{ 1 + \left[ (I_a^2 - I_c^2) / I_c^2 \right] f(r)^2 \right\}^{\frac{1}{2}} \hat{\theta}. \quad (2.68)$$

Above equation represents an expression for magnetic field developed during beam-wave interaction mechanism taking into account Brillouin density profile function that further helps during the spoke formation.

As RBF condition is reached or magnetic insulated sheath is formed between tip of discs and cathode surface, the transient state allows the establishment of the space charge waves along the magnetically insulated sheath. These space charge waves oscillate with plasma frequency. Due to these oscillations, instabilities are developed and RF voltage is induced across the interaction cavity and electrons drift with velocity defined by expression (2.54). This RF voltage is induced due to presence of the radial electric field described by expression (2.53). When synchronism condition is attained, beam-wave interaction starts and under Diocotron instability [Chen (2002)], spokes form due to radial component of electric field and energy transfers occurs due to axial component of electric field. RF energy is stored inside the interaction cavity. To extract RF energy it is necessary to couple the extractor cavity with the output coaxial waveguide. The covering of collector on cathode constitutes an additional cavity which plays an important role in storing the

RF energy generated in MILO, and then transfers this energy to the external load in the form of pulse.

### 2.3 Effect of Axial Periodic Discs on Insulation

Till now, electric and magnetic field profiles describing the magnetic insulation and beam-wave interaction mechanisms process are described. Magnetic insulation establishes space charge RBF equilibrium, thus a stable electron sheath is formed between the metal disc tip and the cathode. It has both radial and axial electric field components in addition to the azimuthal magnetic field component. For HPM oscillator — MILO, axial periodic disc loaded coaxial transmission line is often used as its RF interaction structure to support slow EM waves. The presence of the periodic anode resonators is realized from Figure 2.5, that perturbs the EM field condition of a coaxial transmission line due to the presence of periodic metal discs. Taking into account the discs periodicity, the electric and magnetic fields perturbation is derived in this section. During analysis considering a plasma region (electron sheath) in equilibrium, but when this region is perturbed, associated electrons get perturbed due to periodicity of disc and lead to space charge instability. The axial periodic metal boundary of the structure affect the outer radius of the electron sheath due to presence of radial field components. Considering small perturbations, we presume that

$$\psi = \psi_0 + \psi_1.$$

Perturbation  $\psi_1$  is assumed to have the form,

$$\psi_1 = \sum_{n=-\infty}^{\infty} \psi_n \exp[j(\beta_n z - \omega t)], \quad (2.69)$$

From Floquet's theorem,  $\beta_n = \beta_0 + n h_0$  and  $h_0 = 2\pi/L$ .

Parameters  $h_0$  and  $\omega$  represent mode wave number and angular frequency, respectively. The space harmonics ( $n = 0, \pm 1, \pm 2, \dots$ ) generated due to axial



periodicity of the discs. Magnetically insulated electron sheath will interact with the EM field of the resonator formed between cathode and anode discs. The electromagnetic force around the insulated sheath is equal to time derivative of the magnetic field bounded by surface of insulated sheath. In the cylindrical coordinate system, using Maxwell's equation, as the curl of electric field can be expressed as:

$$\frac{\partial E_r}{\partial z} - \frac{\partial E_z}{\partial r} = -\frac{1}{c} \frac{\partial B_\theta}{\partial t} \quad .$$

On applying Floquet's theorem, the above equation becomes:

$$j\beta_n E_{rn} - \frac{dE_{zn}}{dr} = j\frac{\omega}{c} B_{\theta n} \quad . \quad (2.70)$$

Further, the magnetic field profile due to presence of axial current density can be written using Maxwell's equation in terms of the curl form of magnetic field (its radial and axial components) can be written as:

$$\frac{1}{r} \frac{\partial}{\partial r} r B_\theta = \frac{4\pi}{c} J_z + \frac{1}{c} \frac{\partial E_z}{\partial t} \quad , \quad -\frac{\partial B_\theta}{\partial z} = \frac{1}{c} \frac{\partial E_r}{\partial t} \quad .$$

The effect of structure periodicity in the magnetic field profile can be introduced using (2.69), as:

$$\frac{1}{r} \frac{d}{dr} (r B_{\theta n}) = \frac{4\pi}{c} J_{zn} - j\frac{\omega}{c} E_{zn} \quad , \quad (2.71)$$

$$\beta_n B_{\theta n} = (\omega/c) E_{rn} \quad . \quad (2.72)$$

Now, using convective derivative, Lorentz force condition is written as:

$$\left( \frac{\partial}{\partial t} + v_z \frac{\partial}{\partial z} \right) p_z = -eE_z \quad .$$

Taking partial derivatives, as per exponential variation of the RF field quantities (2.69), we can write:

$$j\zeta_n p_{zn} = eE_{zn} \quad , \quad (2.73)$$

where,  $\zeta_n = \omega - v_{z0}\beta_n$  represents the velocity shifted frequency.

Continuity equation can also written as,

$$\frac{\partial n}{\partial t} + \frac{\partial}{\partial z}(nv_z) = 0 ,$$

And 
$$\zeta_n n_n - n_0 v_{zn} \beta_n = 0 . \quad (2.74)$$

The current density within the insulated sheath can be given as:

$$J_z = -en v_z \eta \delta(r - r_e) , \quad (2.75)$$

where,  $\eta = |I_e| / (2\pi r_e n_0 e v_{z0})$  is the normalization constant,  $I_e$  represents total current and  $\delta(r - r_e)$  is Dirac-delta function. Due to perturbation, the space harmonic components of the current density and momentum can be written as:

$$J_{zn} = -e\eta (n_0 v_{zn} + n_n v_{z0}) \delta(r - r_e) , \quad (2.76)$$

and 
$$p_{zn} = m(\gamma_n v_{z0} + \gamma_0 v_{zn}) , \quad (2.77)$$

where,  $v_{z0}$  is the electrons velocity during magnetic insulation and  $v_{zn}$  represents perturbed axial velocity (due to the space charge wave). The presence of perturbed charge density in turn will also perturb the relativistic factor  $\gamma = \gamma_0 + \gamma_1$

where, 
$$\gamma_0 = \gamma\{v_{z0}\}, \quad \gamma_1 = \left( v_{zn} \frac{d\gamma}{dv_z} \right)_{v_z=v_{z0}} .$$

To obtain  $\gamma_n$  expand  $\gamma\{v_z\}$  in Taylor's series about  $v_{z0}$  and retaining only first order terms yield:

$$\gamma\{v_z\} = \gamma\{v_{z0}\} + \left( v - v_{z0} \right) \frac{d\gamma}{dv_z} \Big|_{v_z=v_{z0}} + \dots .$$

Considering expression for the relativistic mass factor,

$$\gamma = \left( 1 - \frac{v_z^2}{c^2} \right)^{-1/2} ; \quad \left\langle \frac{d\gamma}{dv_z} \right\rangle_{v_z=v_{z0}} = \frac{v_{z0} \gamma_0^3}{c^2} .$$

Similarly,  $n$ th component of perturbed momentum, 
$$\gamma_n = \left( v_{zn} \frac{d\gamma}{dv_z} \right)_{v_z=v_{z0}} .$$

Substituting value of  $d\gamma/dv_z$ , above expression can be written as:

$$\gamma_n = \frac{v_{zn} v_{z0} \gamma_0^3}{c^2} .$$

Now substituting value of  $\gamma_n$  in Equation (2.77), expression for perturbed momentum is written as:

$$p_{zn} = m v_{zn} \gamma_0^3 . \quad (2.78)$$

Further, substituting Equation (2.78) in (2.77), after rearranging is written as:

$$v_{zn} = -j \frac{eE_{zn}}{m \gamma_0^3 \zeta_n} . \quad (2.79)$$

In order to get the perturbed beam current density, Equation (2.74) is solved for  $n_n$  and substituting this value and Equation (2.79) in (2.76), one obtains:

$$J_{zn} = j\eta \frac{e^2 n_0}{m \gamma_0^3} \frac{\omega E_{zn}}{\zeta_n^2} \delta(r - r_e) . \quad (2.80)$$

The radial electric field  $E_{rn}$  is obtained from Equation (2.72) by eliminating  $B_{\theta n}$  with the help of Equation (2.70) as:

$$E_{rn} = \frac{jk_n}{\zeta_n^2} \frac{dE_{zn}}{dr} , \quad (2.81)$$

where,

$$\zeta_n^2 = \frac{\omega^2}{c^2} - k_n^2 .$$

Now, the azimuthal magnetic field  $B_{\theta n}$  is obtainable from Equation (2.70) by eliminating  $E_{rn}$  with the help of (2.81) as:

$$B_{\theta n} = j \frac{\omega}{c \zeta_n^2} \frac{dE_{zn}}{dr} . \quad (2.82)$$

Then the relationship between radial electric and azimuthal magnetic fields is obtained using Equations (2.81) and (2.82):

$$E_{rn} = \frac{c(\beta_0 + nh_0)}{\omega} B_{\theta n} . \quad (2.83)$$

Equating Equations (2.36(b)) and (2.83), then rearranging resulting expression using Equation (2.68) results in expression for critical magnetic field along the insulated sheath for disc loaded coaxial waveguide structure as:

$$B_c = \left( \frac{\mu_0 I_{cr}}{2\pi r} \right) \left\{ 1 + \left[ (I_a^2 - I_c^2) / I_c^2 \right] f(r)^2 \right\}^{1/2} \frac{(\beta_0 + nh_0) \cosh(sr_e)}{\omega \sinh(sr)} . \quad (2.84)$$

Considering RBF or insulation condition, calculate expression for self azimuthal magnetic field that can be written as:

$$B_{\theta}\{r\}=[n_e\{r\}m_e / \epsilon_0]^{1/2} .$$

Substituting above expression in Equation (2.83), and using expression for radial electric field from (2.63(b)), then rearranging results in expression for critical current:

$$I_{cr} = \left[ \frac{n_e\{r\}m_e}{\epsilon_0} \right]^{1/2} \left[ \frac{\cosh(sr_e)}{\sinh(sr)} \frac{\beta_n}{\omega} \right] (2\pi r_c \epsilon_0 c^2) . \quad (2.85)$$

Expression (2.85) represents relation for the critical current of a disc loaded coaxial structure.

## 2.4 RESULTS AND DISCUSSION

In above sections considering coaxial transmission line, condition for RBF has been explained in conjunction with magnetic insulation condition. Using above defined mathematical expression, effect of disc-loaded coaxial waveguide as RF interaction structure in MILO due to presence of electron sheath between tip of disc and cathode has also been analyzed. During analysis, mathematical expressions describing the behavior of radial and axial electric and magnetic field profile to investigate the MILO oscillation condition are also discussed. The magnetically insulated flow condition of MILO device describes the existence of an unstable field of slow space charge wave causing stable oscillation condition for the device. Considering these expressions and implementing programming software, condition at which magnetic insulation occurs is explained using figures mention in this section.

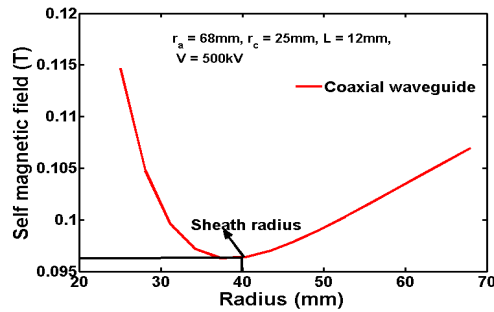
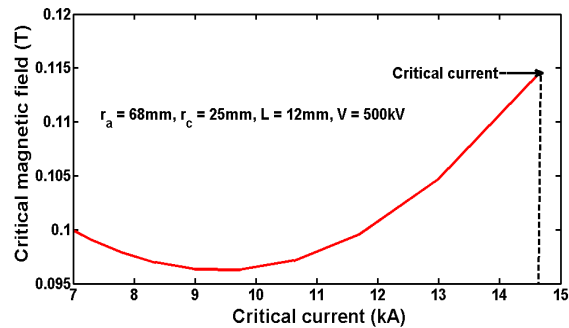
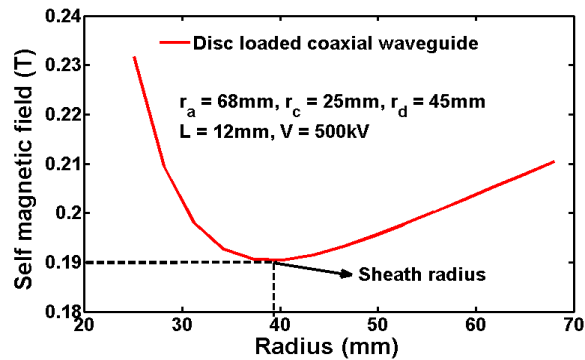


Figure 2.11: Exploration of sheath radius due to variation of self magnetic field.

In MILO, magnetic insulation condition occurs when critical magnetic field become equal to self azimuthal magnetic field. In order to describe the behaviour of self magnetic field generated inside the coaxial structure and disc loaded coaxial structure, for the electromagnetic analysis of the structure, here results obtained using mathematical analysis are plotted for typically chosen structure and beam parameters, where radius of anode ( $r_a = 68$  mm), radius of cathode ( $r_c = 25$  mm), periodicity between discs ( $L = 12$  mm) and are shown in Figures described below. Figure 2.11 explains about the self magnetic field developed during magnetic insulation process at which sheath radius is formed for coaxial waveguide. Figure 2.12 explains nicely about critical current at which magnetic insulation takes place in case of coaxial waveguide.



**Figure 2.12:** Variation of critical magnetic field with critical current for coaxial waveguide.



**Figure 2.13:** Exploration of sheath radius during magnetic insulation process.

For disc loaded coaxial waveguide that acts as an RF interaction structure for HPM devices, amount of sheath radius formed during magnetic insulation can be inferred from Figure 2.13. It is inferred from Figure 2.14 that after certain minimum magnetic field, an electron sheath is formed between tip of discs and cathode at a certain critical current for defined structural parameters. For the validity of the approach developed here, for the EM analysis of this structure, as a special case when disc hole radius becomes equal to anode radius, analysis of disc-loaded waveguide converts into coaxial waveguide as shown in Figure 2.14.

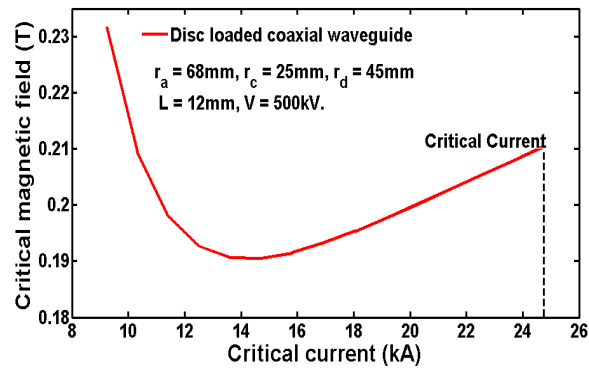


**Figure 2.14:** Determination of critical current due to variation of critical magnetic field.

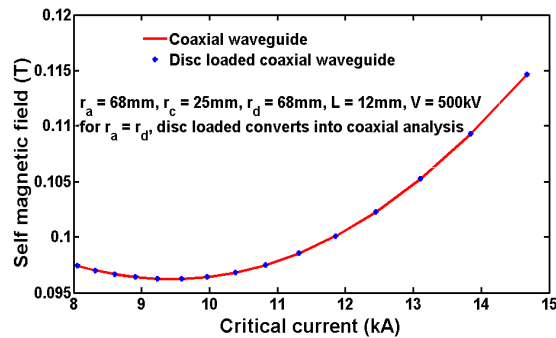


**Figure 2.15:** Plot describing variation when disc-hole radius becomes equal to anode radius.

It can be inferred from above figures that electrons drift axially between tip of discs and cathode due to amount of generated self azimuthal magnetic field. Amount of self magnetic field generated helps in confining electron sheath between tip of discs and

cathode. This analysis could be extended further for beam-wave interaction analysis in HPM devices.

## **2.5 CONCLUSION**

Electromagnetic analysis of coaxial and disc-loaded coaxial waveguide structure is performed, considering case of the HPM devices. Mechanism of self magnetic insulation has been described in detail considering process of explosive emission from the surface of cathode, that is related to generation of plasma frequency in high power microwave devices. Set of equations that describes relativistic Brillouin electron flow in cylindrical coordinates is presented. Considering RBF conditions, expressions describing the behaviour of self magnetic field has been explained in different sections for both coaxial and disc-loaded coaxial waveguide. These expressions have provided knowledgeable insight for understanding the basic physics for understanding operation of MILO.